SANDIA REPORT
SAND2001-1523
Unlimited Release
Printed June 2001

Real-time Visualization and Pressure Diagnostics for Neutron Generator Encapsulation

Cecily A. Romero

Prepared by
Sandia National Laboratories
Albuquerque, New Mexico 87185 and Livermore, California 94550

Sandia is a multiprogram laboratory operated by Sandia Corporation, a Lockheed Martin Company, for the United States Department of Energy under Contract DE-AC04-94AL85000.

Issued by Sandia National Laboratories, operated for the United States Department of Energy by Sandia Corporation.

Available to DOE and DOE contractors from
U.S. Department of Energy
Office of Scientific and Technical Information
P.O. Box 62
Oak Ridge, TN 37831

Telephone: (865)576-8401
Facsimile: (865)576-5728
E-Mail: reports@adonis.osti.gov
Online ordering: http://www.doe.gov/bridge

Available to the public from
U.S. Department of Commerce
National Technical Information Service
5285 Port Royal Rd
Springfield, VA 22161

Telephone: (800)553-6847
Facsimile: (703)605-6900
E-Mail: orders@ntis.fedworld.gov
Online order: http://www.ntis.gov/ordering.htm

SAND2001-1523
Unlimited Release
Printed June 2001

Real-time Visualization and Pressure Diagnostics for Neutron Generator Encapsulation

Cecily A. Romero
Engineering Sciences Center
Sandia National Laboratories
P.O. Box 5800
Albuquerque, New Mexico 87185-0836

Abstract

Experiments were conducted using an approximate model of the MC4380 neutron generator to obtain data on the encapsulation process for this component. Visual data (video) and transient pressure traces were collected. The purpose of the experiments was to provide preliminary validation data for modeling encapsulation mold-filling processes using the GOMA finite element fluid dynamics code. Both particle-free and particle-filled fluids were used to provide data for varying levels of computational complexity. This report gives a review and interpretation of the experimental results, and suggestions for GOMA validation activities.

Acknowledgements

This work was carried out under FY00 MAVEN funding for Neutron Generator Encapsulation (Lisa Mondy, project manager). Rocky Erven provided support in shop work. Tim O'Hern provided the Kalliroscopic® fluid and the laser light sheet. Laboratory space and video imaging equipment were provided by John Emerson and Org. 14172. Howard Arris provided the fillers and assistance in mixing the suspensions. Kim Shollenberger provided the Validyne pressure hardware.

Contents

Figures

1 Background and Introduction

In support of Sandia's neutron generator manufacturing obligation, work within Center 9100 has been continuing to develop modeling and simulation capabilities for the process of encapsulating the neutron generator. The critical reliability issues associated with this component require a detailed understanding of the manufacturing process and its relation to factors such as resulting particle concentration profile. The lower portion of the unit, the power supply (MC4368), is encapsulated in an epoxy loaded with aluminum oxide (ALOX). The upper portion of the unit, the neutron tube (MC4277), is encapsulated in an epoxy loaded with glass microballoons (GMB). In the encapsulation process, the particle-loaded mixture flows into a mold containing the neutron generator. First the ALOX-loaded suspension is introduced to the level just above the power supply as indicated in Step 1 below. The GMB-loaded suspension is then immediately introduced through the same port to encapsulate the rest of the unit (Step 2). The part is then cured according to a temperature schedule optimized for the given epoxy system.

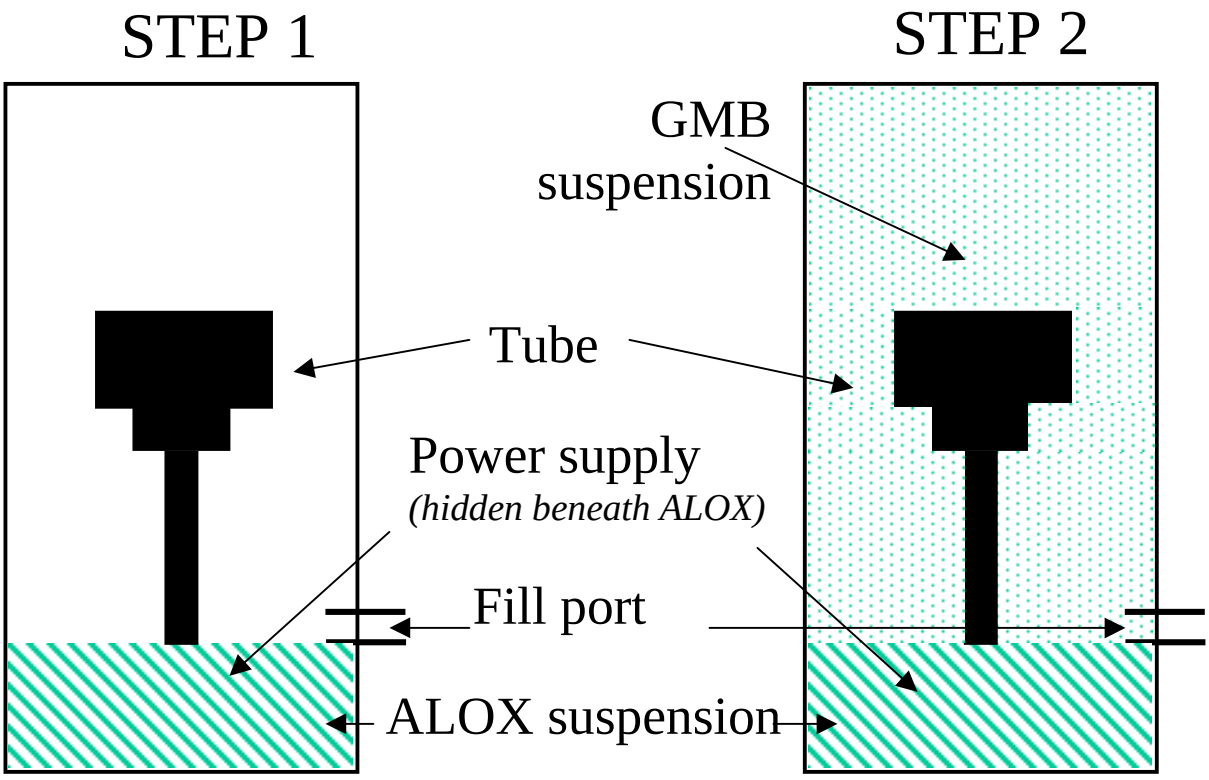

Figure 1. Encapsulation Process

The finite element code, GOMA [1], solves the general Navier Stokes equations and, with the correct constitutive models for hydrodynamic diffusion, can simulate the motion of fluid and migration of particles during the mold filling and subsequent early curing. Density differences between the particles and the entraining fluid can cause particle migration prior to curing. Shear gradients introduced in a flowing suspension can also cause migration of particles across streamlines [2] and, in particular, when the particle loadings (volume fractions) of suspensions exceed 0.4, such as is the case for the neutron generator encapsulants, the effect of a shear stress gradient can, in fact, dominate the flow [3]. Various methods of incorporating the physics of shear enhanced particle migration, and hindered settling behavior of suspensions are in the literature [4,5]. The GOMA development team is working to incorporate the suspension physics into the finite element code.

This work was undertaken to provide experimental validation data for the neutron generator mold fill process. A Lucite™ model of the MC4380 neutron generator that was manufactured by the Neutron Generator Manufacturing Department, was used in this work. This component is unclassified but the neutron tube region is similar in shape to the production component MC4277. The power supply portion is replaced by a stem to support the unit. The mold and mock component have been meshed for use by GOMA,

Figure 2. Photograph of mock neutron generator (left). Finite element mesh of mock neutron generator mold space (right)

as shown in Figure 2.

Validation of GOMA's treatment of suspension flow can be strengthened by comparing experimental results and simulations of identical geometry. Additionally, flow visualization in a geometry similar to the actual component may provide insight into the phenomena occurring in the production process.

2 Instrumented Mold-Fill Experiments

Relevant dependent variables during the brief period of filling the mold include the velocity field, pressure field, and particle concentration distribution. Transient pressure profiles at three locations and visual data were collected for pure fluids and suspensions under carefully controlled conditions. The series included these experiments:

1. Particle-free single fluid encapsulating the entire component
2. Particle-free lower fluid pre-fill, followed by encapsulation with lower density, particle-free fluid
3. Matched index-of-refraction fluid-particle system

In the sections to follow, the experimental apparatus and data collection procedures are described, and experimental results are presented and discussed for each class of experiments.

2.1 Experimental Apparatus

The experimental apparatus consisted of a mold assembly, a vacuum pump, pressure transducers, a video camera, and two PCs for data/video collection. At the core of the apparatus is the mock neutron generator, approximating the actual MC4380 but with

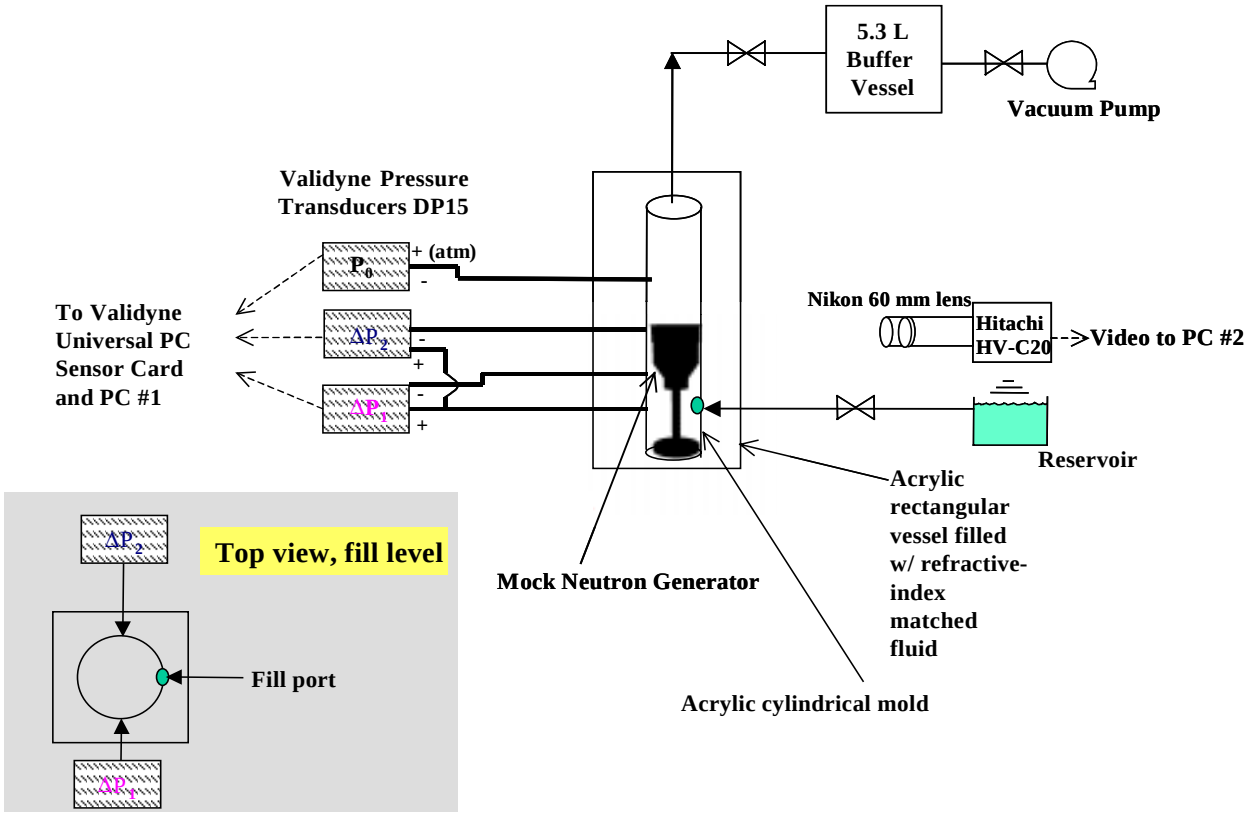

Figure 3. Experimental Apparatus Schematic

simplified geometry, so that the part is unclassified, and more easily meshed and modeled in GOMA than the real, more complex geometry. The schematic is shown in Figure 3.

Typical encapsulation experiments were performed as follows: A vacuum pump was used to purge the mold prior to filling. The mold fill was accomplished by filling a funnel (fluid reservoir in Figure 3) with the encapsulant fluid, in line with a valve to the mold fill port. When the valve was opened, the pressure differential between the atmospheric fluid and the evacuated mold drives the fill process. This is the same as the driving force used in production. During the mold fill, video was recorded, and pressure data were collected, as described next.

Video

It was desired to collect a qualitative image of the flow field for this series of experiments. To accomplish this for the particle-free fluids, two steps were taken. First, a small amount of Kalliroscopic® fluid (AQ-1000 rheoscopic concentrate) was added to the fluid prior to filling. This material provides tracer particles that could be tracked to provide transport data (e.g. local velocities) during mold filling. Secondly, a laser light sheet (using a Class II Helium-Neon laser) was directed to a vertical plane within the mold, about one inch above the fill port. This light sheet helped to accentuate the tracer particles in the plane of interest. A Hitachi HV-C20 3CCD video camera equipped with a 60 mm Nikon lens was used to collect video data, captured at 10 frames per second using Adobe Premier video capture software. The camera could be focused either in a small region (e.g. at the laser light sheet), resulting in a focal area of approximately 4 cm^2, or it could be focused over a larger area (e.g. 25 cm^2). The video images were used to qualitatively assess the mold filling process. Although not performed in this study, more quantitative velocity results could be derived from some of the videos using Particle Image Velocimetry (PIV) analysis. It was not believed the data obtained warranted this more exhaustive (complete) study at this time.

The Lucite™ mock neutron generator was placed within a cylindrical acrylic mold, 4.45 cm (1.75 inches) inside diameter. This assembly was placed within a larger rectangular acrylic vessel as shown in Figure 3. The space between the rectangular vessel and the cylindrical mold was filled with a fluid of the same index of refraction as the encapsulation fluid to eliminate the distortion in the radial direction caused by the interface of the curved walls of the mold and air. Figure 4 illustrates the effect of the fluid on reducing the radial distortion. The curved mold interface becomes nearly invisible and the distortion of the graph in the background decreases.

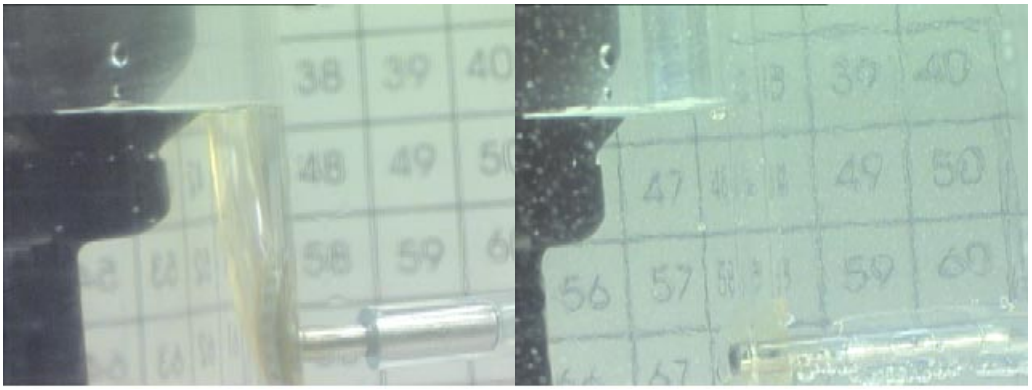

Figure 4. On the left, the mold is shown without the rectangular vessel. On the right, the vessel is used and it is filled with index-matched fluid, minimizing radial distortion due to vessel curvature.

Pressure Measurement

Diaphragm pressure transducers (Validyne DP15) were used at three locations within the mold. One is used to measure the mold pressure relative to atmospheric pressure (the driving force for the mold-fill process, as indicated by P_0 in Figure 3). The other two are used to collect differential pressures between the inlet port and locations 2.54 cm (1 inch) and 5.08 cm (2 inches) above the inlet port, respectively. These positions are indicated in Figure 3 as ΔP_1 and ΔP_2. These locations are referred to as 1" and 2" ports, respectively, in the remainder of this report. Pressure data using these transducers were collected at a channel frequency of 66.67 Hz (5,000 Hz collection frequency with 25 point averaging over 3 channels). A gain of ±80 mV/V was used on all 3 channels. The signals from the pressure transducers were captured by a Validyne Universal PC (UPC) data acquisition card.

A vacuum pump was used to evacuate the mold to obtain the required pressure differential prior to filling. Because of the interference of the pump vibration with the sensitive differential pressure collection, the pump was turned off prior to filling. However, this introduced a new problem of a drop in the mold vacuum as the fill proceeded. To minimize this effect, a vessel (5.3 L) was added between the vacuum pump and the mold. This served as a vacuum buffer, essentially increasing the system volume to minimize pressure variation, which could disturb the experiment. Figure 5 illustrates the improvement in maintaining the vacuum achieved by the buffer vessel.

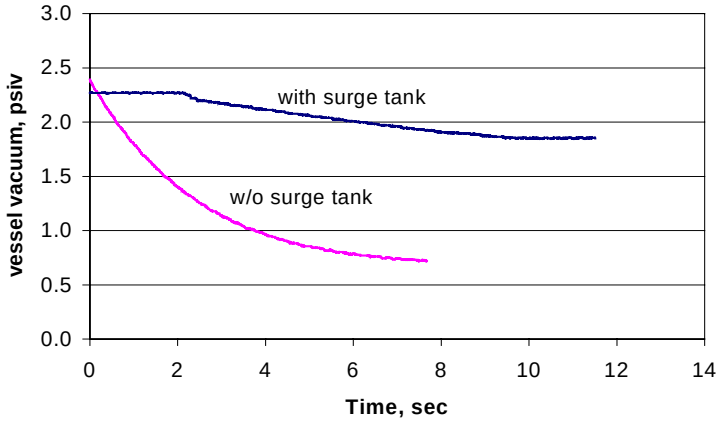

Figure 5. Effect of buffer vessel on mold pressure during typical mold fill

The rectangular vessel discussed previously was equipped with special Swagelock fittings to allow flexible, sealed passage of 0.318 cm (1/8") tygon tubing from the pressure transducers to the mold, as shown in Figure 6. It was necessary to equip the vessel in this way rather than to allow the tubing to come in through the top of the vessel for two reasons: 1) the length of tubing needed to be minimized in order to eliminate distortion due to coupling of the pressure measurement frequency with the natural frequency of the system[1] and 2) very small pressure differentials (on the order of 0.55 kPa, or 0.08 psi) exist in the mold, so even slight elevation changes between the high pressure transducer input and the vessel port resulted in invalid pressure readings due to migration of fluid in the tubing. Any elevation changes would change the pressure reading by the corresponding hydrostatic head.

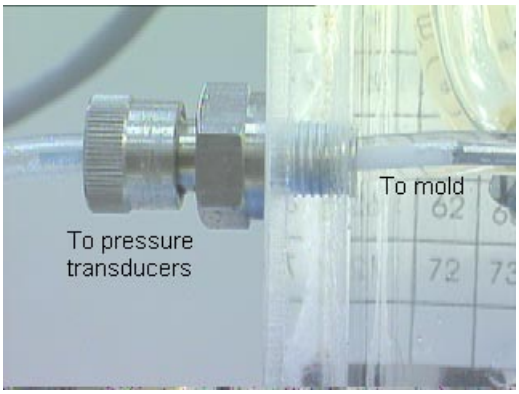

Figure 6. Instrumentation detail

[1] The frequency responses of the long (0.91m, or 36 inch) and short (0.10m, or 4 inch) tubing lengths were calculated as 530 s^{-1} and 4507 s^{-1}, respectively.

The pressure transducers used in this study were variable reluctance pressure transducers, consisting of a diaphragm constructed of magnetically permeable stainless steel, bolted between two blocks of stainless steel. Within each stainless steel block is an inductance coil on an E-shaped core. A physical distortion in the diaphragm due to a pressure difference across it occurs, causing the gap distance between the diaphragm and the legs of each E-core to change, thus changing the inductance of each coil. The change in relative coil inductance is the quantity measured by the transducers [6]. The diaphragms used for the 1" and 2" spans were DP15-20[2] (valid in a range of pressures up to 0.86 kPa (0.125 psi) with an accuracy of ±0.25% full scale, or ±0.00215 kPa (±0.0003 psi)).

The pressure transducers were calibrated periodically during this study. Typical calibration curves are shown in Figures 7 and 8. The transducer outputs increased linearly with pressure, as expected. Calibrations on the differential transducers were conducted by adjusting the fluid head in the vessel with a fluid of known density and observing the static transducer output at each liquid head. Figure 7 gives the direct observations and Figure 8 shows the resulting calibration curve for the transducer that measures the pressure differential between a point level with the fill port and 2 inches above the fill port. As expected, increasing the fluid level above the top transducer port had no influence on the pressure transducer reading.

Calibration of the transducer that measured the pressure inside the mold relative to atmospheric was conducted using a barometer and a Digiquartz® Paroscientific quartz pressure instrument (resolution of 0.1 ppm) for accurate calibration. It was calibrated over the range from atmospheric to the maximum vacuum that could be achieved with the vacuum pump, 1.2 kPa (0.17 psi). The following sections detail the results of the encapsulation experiments.

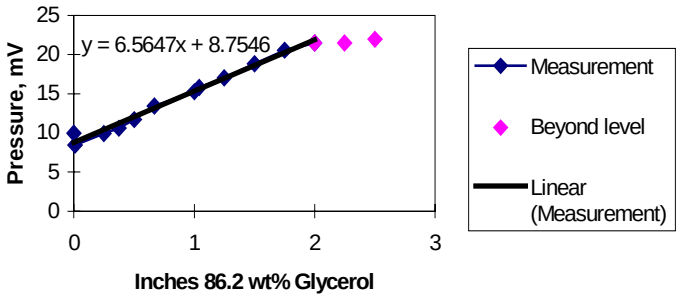

Figure 7. Raw calibration of pressure transducer #1

[2]For experiments prior to 7/13/00, the Diaphragm #2, which was connected to the 1" span, was a DP15-22, which has a broader range, from 0 to 1.38 kPa (0.20 psi). This is noted as an exception where applicable.

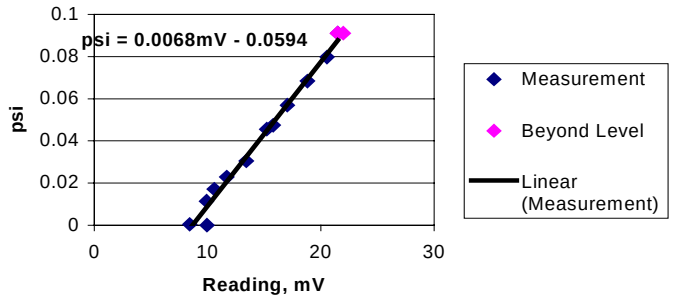

Figure 8. Calibration curve of pressure transducer #1

2.2 Single-fluid Particle-free Mold Fills

Experiments were conducted using single Newtonian fluids with no fillers for the encapsulation as initial validation data for GOMA. A solution of 86.2 wt % glycerol in water was used for several of the runs, while 100% glycerol was used in other runs. The room temperature density and viscosity of these fluids is 1.226 g/ml, 1.27 Poise and 1.261 g/ml, 1.49 Poise, respectively. Both fluids provided reasonably good video imaging. The actual GMB-filled suspension has a viscosity of 10 Poise at the fill temperature of 54°C, and a bulk density of 0.72 g/ml. The Reynolds number (Re) at the inlet fill port for the ideal fluid (those used in the experiments) is equated with that of the real suspension:

$$\frac{\mathrm{Re}_{sus}}{\mathrm{Re}_{id}} = \frac{\bar{u}_{sus}\rho_{sus}\mu_{id}}{\bar{u}_{id}\rho_{id}\mu_{sus}} = 1 \qquad (1)$$

Also, for parabolic flow into the inlet port, the following condition is satisfied:

$$\frac{dP_{id}}{dP_{sus}} = \frac{\bar{u}_{id}}{\bar{u}_{sus}}\frac{\mu_{id}}{\mu_{sus}} \qquad (2)$$

In the above equations, $\bar{u}$ is the average fluid velocity, ρ is the density, μ is the viscosity, P is the pressure, and the subscripts *id* and *sus* denote the ideal fluid and the suspension, respectively. This resulted in a ratio of pressure differentials of 0.01 (the pressure differential scales as viscosity squared). For mold filling of the actual suspension, the pressure in the mold is brought down to about 0.67 kPa (5 mm Hg) absolute, resulting in a pressure differential of about 82.7 kPa (12 psi) for a typical day in Albuquerque. Equating the Reynolds numbers suggested a pressure driving force of 0.83 kPa (0.12 psi) for the 86.2% glycerol/water solution to achieve similar flows[3]. This turned out to be

[3] Assuming a 5-10 second fill time in the actual process, the characteristic Reynolds number at the inlet is on the order of 1-2.

impractical: the rate of fill was extraordinarily slow, and it was not possible to maintain this driving force at a constant value. Consequently, the pressure differential was kept as low as possible, but increased to a level that allowed a reasonable volumetric flow rate. The differential pressure used was typically about 32.4 kPa (4.7 psi). Thus, the filling times were of the same order of magnitude as those used in the real encapsulation process, but due to the much lower viscosity and higher density fluids used in this experiment, the Reynolds numbers were a factor of 40 higher.

Prior to the mold fill experiments, a trace amount of Kalliroscopic® fluid (0.25 volume %) was added to the reservoir. A plane within the flow field was illuminated with a laser light sheet. Figure 9 illustrates a typical series of images from a single-fluid mold fill.

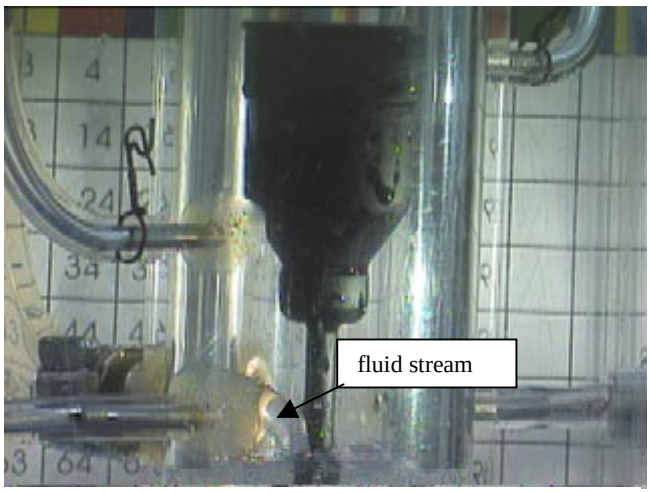

1. Encapsulant enters through fill port

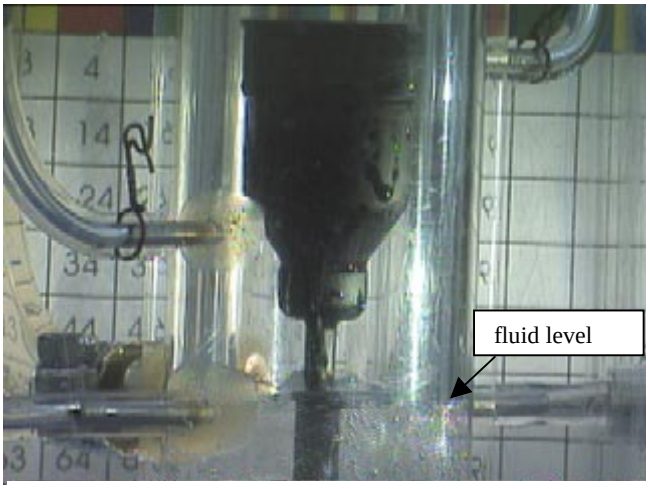

2. Encapsulant reaches fill level

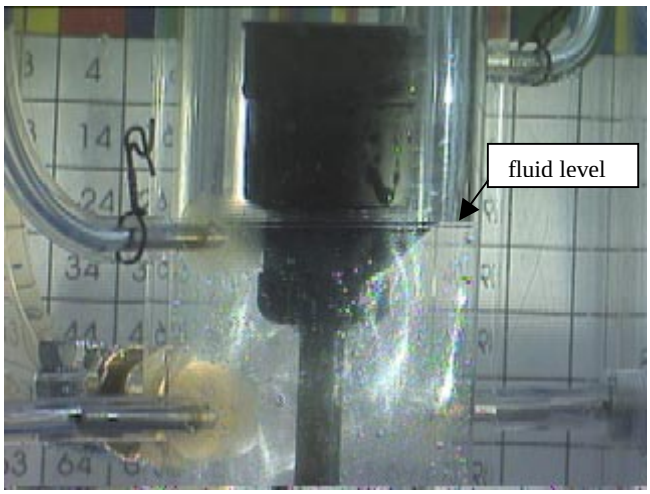

3. Encapsulant reaches 1” level (adjacent to pressure port)

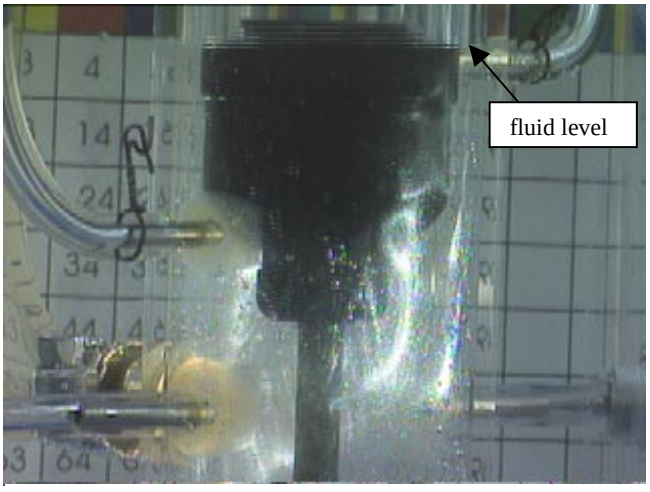

4. Encapsulant reaches 2” level (adjacent to pressure port)

Figure 9. Mold Fill Sequence Illustration

Pressure traces were also obtained during filling. A typical pressure trace is shown in Figure 10, and more single-fluid mold fill pressure traces are given in Appendix A.1. Figure 10 illustrates pressure traces for the case of a solution of 86.7 wt % glycerol in water, doped with a small amount of Kalliroscopic® solution. The differential pressure between the lower pressure port and locations 1-inch (corresponding to ΔP_1 in Figure 3) and 2-inches (ΔP_2) above the lower port, are illustrated as a function of time. The zero time is the time at which the video was begun. The pressure trace was started a few seconds later (3.3 seconds in this case). Some interesting behavior occurred for the majority of the mold fills. A surprisingly lengthy delay between the fluid level reaching

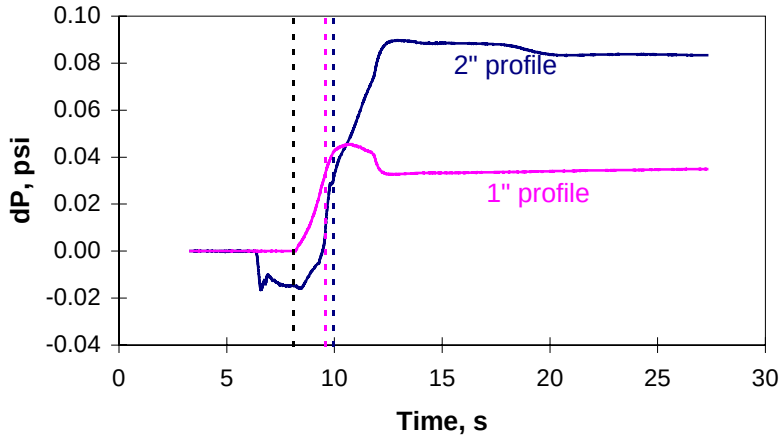

Figure 10. Example pressure trace (Fill7-201) using 86.7 wt% glycerine

the upper transducer port and the recording of the maximum pressure occurred. Several reasons for this behavior have been investigated, including experimental error and physical reasons, which are further explored in the Discussion section. Debugging of the system has found no evidence of experimental errors which could cause this, but no convincing physical reason for the delay is apparent either. Another feature, which is illustrated in Figure 10, is a distinct pressure drop below the baseline just as fluid is injected for the 2" (ΔP_2) profile. The pressure is recovered as the fluid fills above the inlet level. It is possible that this is due to the entrainment of neighboring air as the fluid 'jet' is introduced, causing a decrease in the local pressure. Once the fluid level increases above the level of introduction, the pressure recovers. Interestingly, only the 2" transducer exhibited this behavior. A feature that is unique to Figure 10 is that the pressure on the 1" trace decreased rapidly and then leveled out after it reached its maximum. This was not observed for any other runs. The hydrostatic pressure for a 1" head of this solution is 0.303 kPa (0.044 psi), and 0.606 kPa (0.088 psi) for 2", very close to the observed maxima of Figure 10. Thus, the final measured pressures agree well with predictions but several features of the intermediate behavior remain unexplained. The first part of Appendix A.1 illustrates a number of other single fluid mold fill traces.

2.3 Two-Fluid Mold Fill

The actual neutron generator encapsulation, as described earlier, is accomplished with two separate suspensions. Validation experiments using the same mock mold but with two encapsulant fluids, rather than a single encapsulant fluid, were used and are discussed in the following two subsections.

Particle-filled transparent 2-fluid mold fill

An interesting and potentially important aspect of the mold filling process is that after the ALOX layer is poured, a new suspension loaded with glass microballoons, GMB, is immediately added. The interaction of these two suspensions adds further complexity to the fluid dynamics. The encapsulant suspension used in production is opaque so a surrogate system of suspensions was developed for the purpose of visualizing the GMB (upper) fill over a compatible ALOX (lower) suspension.

Transparent silica particles (Grace Davison Chromatographic Silica Gel, Grade 633N, with $47<a<61$ microns) with an index of refraction, n=1.452, were suspended in a solution of 86.7 wt % glycerol in water, of the same index of refraction. In order to approximate the apparent relative viscosity (μ/μ_0) of the actual (but opaque) GMB suspension, the particle loading was adjusted. It was found that the silica gel absorbed fluid into its interior. Consequently, a particle loading for the silica solution of 3.39 times less than that for a GMB suspension resulted in an equivalent viscosity (to simulate 48 vol % GMB, 12.5 vol % silica was required). Fluid densities were within 2% of one another ($\rho \sim 1.2$ g/cm^3), but the particle densities could not be matched. The GMB density is 0.4 g/cm^3 while the silica density is 2.1 g/cm^3. For the power supply encapsulant, ALOX-loaded epoxy, it was not required to achieve a clear suspension. ALOX was used with 80 wt % glycerol/water (80% was chosen rather than 86.7% to match the viscosity of the simulant fluid at 20^{o}C with the epoxy fluid at 54^{o}C, the pour temperature). Table 1 summarizes the fluid content and properties.

Initial flow visualization experiments using these surrogate suspensions indicated the possibility that the GMB suspension could entrain some of the lower ALOX suspension upon introduction, and deposit it either on the interior mold surface opposite the fill port, or on the internals of the neutron tube. Figure 11 shows the results of these experiments. The fill port is on the rear side of the vessel near the right in this series of photographs. As the upper suspension is introduced, it tends to sweep up some of the lower suspension. This pattern has also been observed in finished pieces by cross sectioning (within Org. 14000).

Table 1 Summary of conditions for mold-fill sequence of Figures 11-13

	Upper Fluid	**Lower Fluid**
Fluid	86.7 wt % glycerol in water	80 wt % glycerol in water
Particles	Chromatographic silica gel, Grace-Davidson, Grade 633N, 47-61 μm	Standard weapon-grade aluminum oxide, ALOX
Index of refraction	1.452 (20°C)	N.A. (particles are opaque)
Particle-free viscosity	127.0 cP (20°C)	59.9 cP (20°C)
Suspension viscosity	10 P (20°C)	15 P (20°C)
Fluid density, g/cm^3	1.226	1.226
Particle loading	12.54 vol% (to simulate 48 vol% GMB loading in epoxy. See next section for discussion)	100:300 (wt fluid:wt filler)

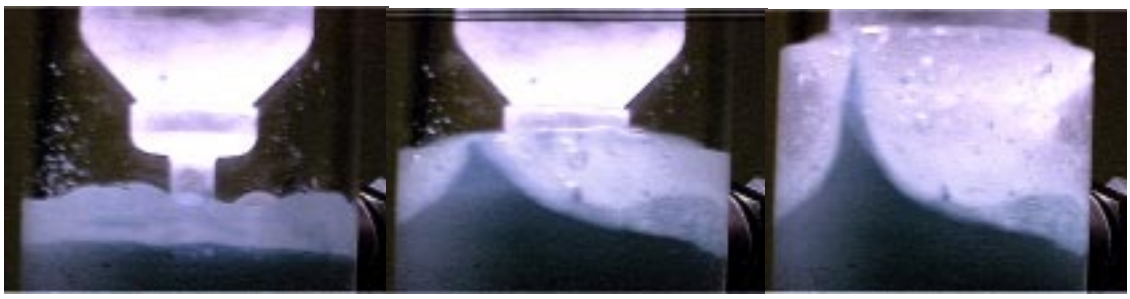

Figure 11. Sequence of mold fill, from FY99

The mold fill experiment that was previously visually observed (Figure 11) was repeated with the pressure instrumentation in place. The same surrogate system of suspensions as summarized in Table 1 was used.

The opaque ALOX suspension was first introduced into the mold, to a level even with the fill port. It was de-gassed for approximately 10 minutes, and then the transparent silica solution was introduced while recording video and pressure profiles. Figure 12 shows the level of pre-fill with the ALOX suspension prior to de-gas and introduction of the upper suspension.

The video and pressure capture was only marginally successful for this experiment. Difficulties occurred with plugging of the transducers and anticipating the correct fill times. Figure 12 shows a pressure trace collected for the initial portion of an ALOX/Silica-loaded fill. The steady but slight decline in pressure could be a consequence of the slight drop in mold pressure as the valve is opened. (See Appendix A.3 for the vessel pressure trace.) This pressure trace only caught a small portion of the

fill[4], as the 1" level was not reached until close to 24 seconds into the mold filling experiment. The corresponding hydrostatic pressure would be 0.331 kPa (0.048 psi) for the suspension at the 1" level. A linear approach to this state is indicated by the long dashed line in Figure 13. The slope is consistent with the observed initial slope. Because the silica-loaded suspension is likely to behave differently from the GMB used in the actual encapsulation, due to its porosity and non-spherical shape, it was not pursued further. The next section discusses more details of all three classes of experiments and gives suggestions for obtaining data for particle-loaded suspensions with properties much closer to that of the actual epoxy encapsulants.

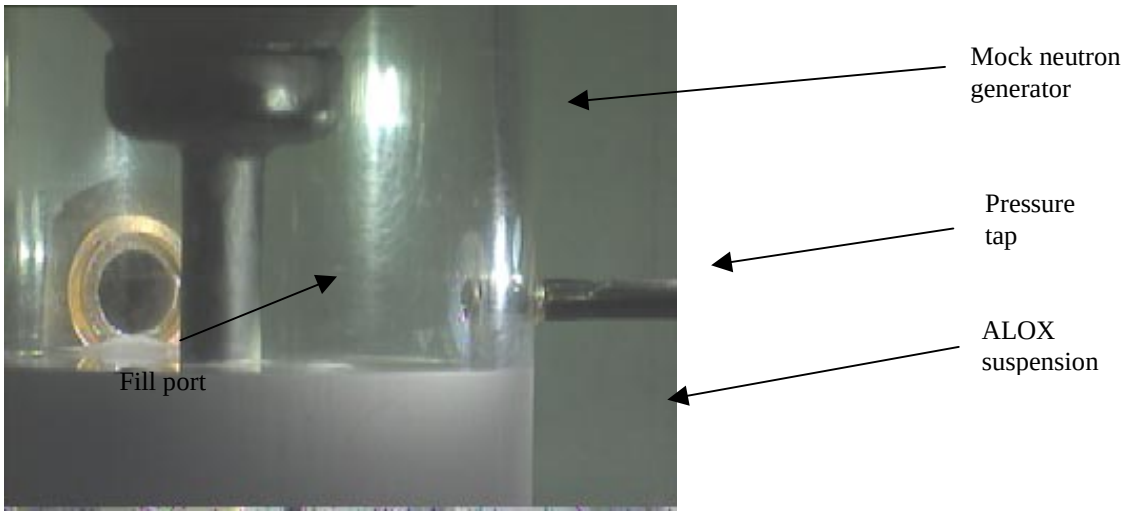

Figure 12. The ALOX suspension is prefilled to just below the fill line inlet

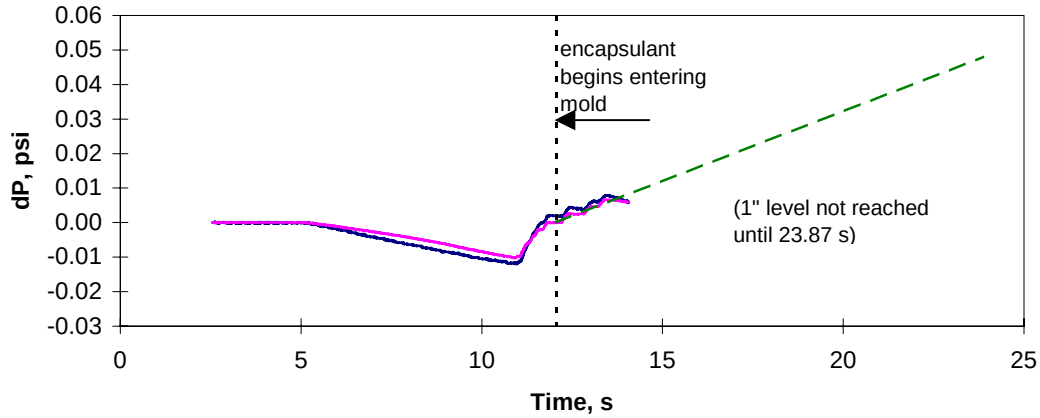

Figure 13. Partial pressure trace (see footnote) for particle-filled mold fill using 86.7 wt % glycerol and ALOX (bottom layer), SiO_2 (top layer). The dashed line shows the expected progression to 0.331 kPa (0.048 psi) at 23.87 s.

[4] The duration of data collection is pre-selected and the extraordinarily long time for this thick suspension

Particle-free two-fluid mold fill

A more quantitative study of the effect of mold filling over a pre-existing, stagnant layer, was replicated, without particle loading, primarily for validation exercises. Two fluids, of differing densities were used. It wasn't possible to exactly replicate the true bulk density difference. The GMB-loaded suspension has a density of only 0.72 g/cm^3, due to the low density of the glass balloons, whereas the density of the ALOX (3.93 g/cm^3) results in a bulk density of 2.39 g/cm^3 for the ALOX suspension. No combination of particle-free transparent fluids could be found to give this density ratio. For the purpose of validating the encapsulation process using GOMA, however, two fluids of differing densities were used, the heavier fluid beneath the lighter. The lower fluid used was a mixture of UCON HB 90,000 with tetrabromoethane, with a resulting density of 1.473 g/cm^3 at 22^{o}C (measured using a Mettler densitometer), and a viscosity of 73.5 cP at 25^{o}C (measured using a Canon-Fenske viscometer). The upper fluid was 100% glycerol with a density of 1.26 g/cm and a viscosity of 17.63 P at 20^{o}C.

Figure 14 gives an example pressure trace for the mold fill, beginning with the lower level pre-filled to the inlet port. More data from two-fluid fills are provided in Appendix A.2. Meaningful data could only be collected from one of the transducers (the 2-inch span) for this run, although the one-inch span transducer did respond to a pressure spike that was purposely introduced into the system as a reference point. The working transducer exhibited a large degree of noise, as is obvious in Figure 14. For reference, a static head of 2 inches of fluid (100% glycerol at 20^{o}C) corresponds to a pressure of 0.627 kPa (0.091 psi). No dip in pressure on introduction of fluid just above the pre-filled layer was observed for this series of experiments, unlike the previous (single fluid) experiments. This behavior is consistent with the explanation that the dip is due to local entrainment of air. (It only occurs when the jet is surrounded by air.)

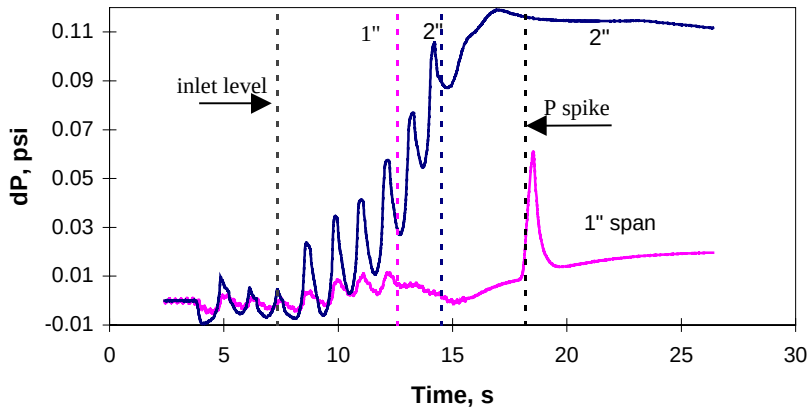

Figure 14. Example pressure trace for 2-fluid particle-free mold fill

to begin entry into the vessel was not anticipated.

Video images showed that entrainment of the pre-existing, denser, stagnant layer did occur. Figure 15 shows an example still image of the entrainment. The clear fluid enters from the lower left (the dark area in Figure 15), above a stagnant layer of heavier fluid, which can be seen on the lower right of the slightly tilted image in Figure 15 (the mold was not tilted, only the image). A ribbon of the previously stagnant lower (dark) fluid is lifted to the right of the mock neutron generator. This is consistent with the behavior observed in the particle filled simulant suspension and in the actual mold fills, although the momentum of the entering fluid is less in this case, and the ribbon of fluid is not carried all the way to the opposite wall.

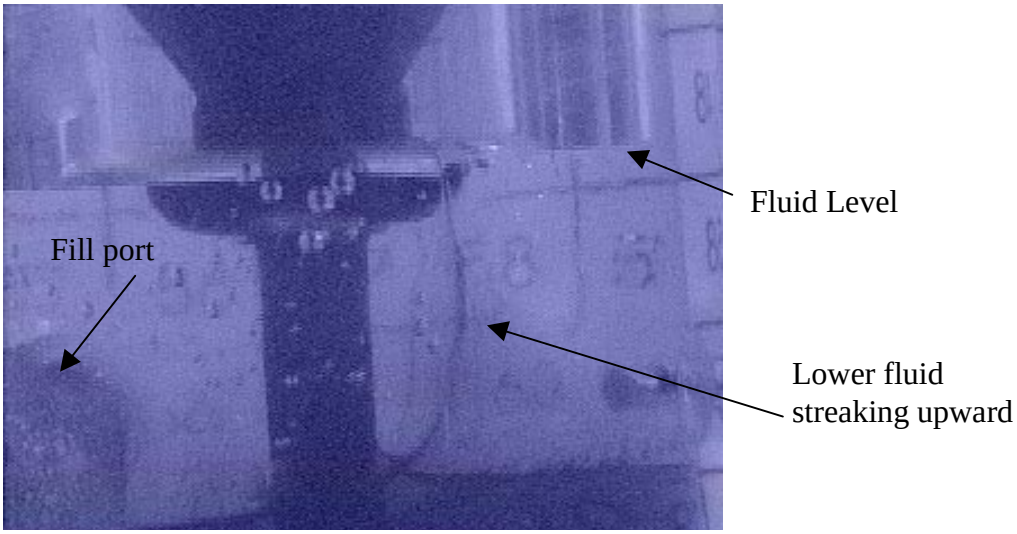

Figure 15. Captured image midway through 2-fluid fill. Note the streak of fluid to the right being lifted by the incoming fluid

3 Discussion

Three classes of mold-fill systems have been described in the foregoing sections. These systems range from a relatively low level of complexity, from a code validation point of view, and progress to a complex system more closely representative of the actual mold-fill system used in the neutron generator encapsulation process. The first and simplest class involves a single, particle-free, nearly Newtonian fluid of relatively low viscosity. The driving pressure gradient and the fill fluid properties were varied. Details of these experiments can be found in Appendix A.1, and the first three figures of Appendix A.4. (The videos are also available separately.) The second class of mold fill systems is similar to the first, except that a less dense particle free, nearly Newtonian fluid is introduced over a stagnant, higher density fluid. This was done in order to obtain validation data that incorporates the added complexity of introducing a less dense fluid over a stagnant, dense fluid layer, while maintaining the simplicity of particle-free, nearly Newtonian fluids. For each of these experiments, the driving pressure gradient and the

fluids were kept the same, to provide a measure of repeatability. See Appendix A.2, and the Figures 7-121, 8-111, and 8-112 of Appendix A.4, along with video for details. Finally, the highest level of complexity involved a 2-fluid system with both fluids particle-filled. These particle-filled fluids are highly non-Newtonian and not well characterized. The particle filler used in the flowing phase is porous, non-spherical silica to provide a transparent fluid, and is particularly difficult to characterize. A much higher driving force was required to cause this suspension to flow. Because the prospects for characterizing this highly non-ideal system are dim, the 'validation data' are probably best used as a qualitative comparison of particle-free vs. particle-filled systems, rather than as quantitative data for this single most complex experiment. A single partial mold fill is provided in Appendix A.3, the last figure of Appendix A.4, and the movie 6-71.avi.

General qualitative trends in observations of the mold fill experiments are:

1. The fill fronts were reasonably flat. That is, the mock neutron generator did not cause significant perturbations in the leading edge of the fluid as it was filling.
2. The effect of viscosity was strong, as evidenced by a much longer fill time for the more viscous 100% glycerol compared to the diluted glycerol solution (compare Fill 7-201 with Fill 7-131 in Appendix A.4).
3. During the two-fluid mold fills, the upper fluid induced motion in the stagnant lower fluid, and, in fact, caused a significant lifting of the lower fluid up into the upper fluid. This is apparent in Figure 11 (particle-filled) and Figure 15 (particle-free).

For each experiment, as video was captured, data from the pressure transducers was continuously collected. Some lag (up to about 2 seconds) often occurred between the arrival of the fluid at a level of the transducer's negative port and the point of maximum pressure. This can be seen in Figure 10 for a single fluid fill and in several pressure traces in the Appendix for both single fluid and 2-fluid mold fills. The reason for this is not clear. The possibility of an interference between the natural frequency of the tubing and that of the transducer diaphragms was minimized by shortening the system tubing length. The estimated frequency response of the tubing was increased from 530 s^{-1} with the original 0.91 m (36 inch) long tubing to 4500 s^{-1} when 10.2 cm (4 inch) long tubing was used instead.

In order to determine if the delay in reaching the peak pressure was real or due to an experimental artifact, the system was perturbed with step functions, by suddenly increasing the pressure. A syringe was used to deliver a sudden pressure increase to the tubing connected to the positive port with the other port at atmospheric pressure. A stopwatch was used to record the time of the increase. Figure 16 illustrates the results of this test. The pressure response is relatively prompt; the transducer registers the pressure spike without significant lag time.

The possibility that the pressure lag may be of physical origin was also investigated. If energy other than static head were significant, then there could be an increase in pressure non-coincident with the arrival of the fluid at the top sampling port of the transducer. For

instance, a fluid flowing through an expansion will result in a conversion of kinetic energy into higher pressure. However, order of magnitude calculations show that the total kinetic energy available during a typical mold fill is only on the order of 1% of the static pressure differential due to fluid head. In any event, there is a constriction, not an expansion in the flow region between the lower port and the upper port. Therefore, the observed lag between the arrival of fluid at the upper transducer port and the occurrence of maximum pressure remains unexplained. Pressure traces are presented here with the zero value adjusted to coincide with the video data collection times, uncorrected for any shift due to instrumentation since this could not be quantified.

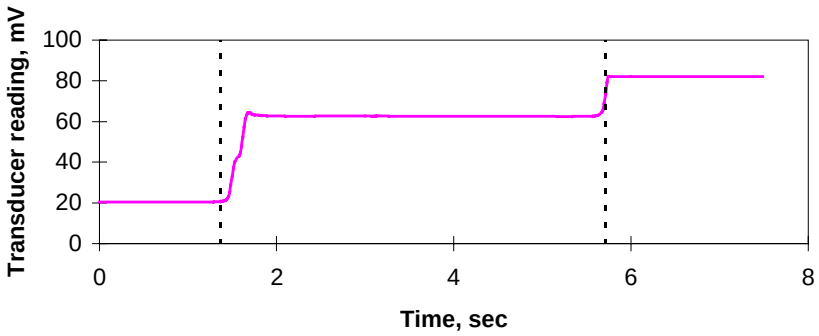

Figure 16. Coordination of pressure transducers with input. The dashed lines indicate recorded times at which the valve was opened.

Another interesting phenomenon occurred during single-fluid fills. Frequently, the differential pressure was observed to dip as the stream of fluid entered the vessel. This is characteristic of the "Bernoulli" effect, the jet of fluid entering entrains the local air, causing a local decrease in pressure. Interestingly, this phenomenon was observed only at one of the ports. When the instrumentation was switched from one port to the other, the dip was repeated at the same physical location. Examples of this behavior are shown in Figure 9 and in several single-fluid fills in the Appendix A.1. The phenomenon did not occur when the mold was pre-filled with a second fluid up to the fill line, consistent with this explanation.

Attempts were made to conduct a mold fill with a system very similar to the actual epoxy/GMB, epoxy/ALOX encapsulant (for the "Z-replacement", 459 system). Ideally, it was desired to avoid using the catalyst, so that no curing would take place. If curing occurred, the mock neutron generator and mold would probably not be salvageable. Therefore, a search for a fluid of properties similar to the ankamine/jeffamine mixture that is the curing agent in the 459 system was undertaken. A mixture of light weight mineral oils of the proper viscosity at the fill temperature of 54^{o}C was found (29.2 vol% DRAKEOL 5, balance DRAKEOL 10). Unfortunately, this mixture formed an emulsion with the 459 epoxy, due to its limited solubility. When mixed with ALOX filler, it was qualitatively very different from the actual suspension [7]. It was decided not to pursue

this experiment at this time since the identification of a non-reacting substitute could be a lengthy process. The 826 resin is neither strictly oil-soluble nor water-soluble. Moreover, it may be prudent to determine the utility of the transient pressure profiles and video of the idealized mold fills to determine if further data on the "real" suspension is warranted. Should an experiment with the true materials (or with an inert substitute for the catalyst) be conducted, the apparatus should be placed in close proximity to the preheat ovens to maintain the temperature near the preheat temperature of 54^{o}C. All materials that will come into contact with the suspension need to be preheated, tubing lengths minimized, and design should allow for rapid connection of instrumentation. Also, the tubing length from the reservoir to the inlet needs to be minimized, and only pinch valves used.

4 Conclusions and Recommendations for Future Activities

The data in this report, along with the video capture of the mold fill experiments, can serve as preliminary validation test cases for GOMA, primarily for the particle-free system (with and without a lower level pre-filled). A complete compilation of the movies and pressure data is available from the author upon request.

The initial validation activities could simply attempt to match the observed free surface locations as a function of time with the actual geometry (see Appendix A.4). The glycerol/water solutions are near-Newtonian, allowing for simple physics, but rather complex geometry, a good starting point for code validation. The corresponding measured pressure driving forces can be treated as a user-defined boundary condition, or, in many cases, a constant pressure driving force may be adequate.

A suggested second level of validation activity from this study is to attempt to numerically replicate the qualitatively observed lifting of the lower, more dense, stagnant layer in the two-fluid fill experiments. Successful replication of this effect in a particle-free system is a logical precurser to the ability to accurately simulate the encapsulant mixing in the actual filled system.

The differential pressure traces that were collected in this work may not be useful for validation purposes. Unexplained behaviors, including slow approach to equilibrium and occasional noisy signals, decrease the confidence in these results. Although the pressure diaphragms used in this work are designed to measure the expected pressure differentials on the order of 0.005 atm, system disturbances and drops of fluid reaching the diaphragm surfaces may cause variations of the same order of magnitude as the pressure differentials that were intended to be measured.

In any case, more useful validation data may be the velocity vectors (in unfilled and filled systems) and particle concentration profiles in filled systems. These quantities more directly relate to the performance of the neutron generator, and are better validation criteria for the constitutive models of shear enhanced particle migration. Future validation experiments should be planned with a careful consideration of the difficulty of obtaining pressure data relative to the value of the pressure information. A focus on the

flow field and particle distribution using Particle Image Velocimetry (PIV), for example, may provide more valuable validation data.

5 References

1. Schunk, P.R, P.A. Sackinger, R.R. Rao, K.S. Chen, R.A. Cairncross, T.A. Baer and D.A. Labreche, 1997 “GOMA 2.0-A Full-Newton Finite Element Program for Free and Moving Boundary Problems with Coupled Fluid/Solid Momentum, Energy, Mass, and Chemical Species Transport: User’s Guide”, Sandia Technical Report, SAND97-2404.
2. Eckstein, E.C., Bailey, D.G. & Shapiro, A.H. 1977 “Self-diffusion of particles in shear flow of a suspension” *J Fluid Mechanics* **79** p. 191-208.
3. Leighton, D.T. & Acrivos, A. 1987 “The shear-induced migration of particles in concentrated suspensions” *J Fluid Mechanics* **181** p.415-439.
4. Nott, P.R. and Brady, J.F., 1994 “Pressure-driven flow of suspensions: simulation and theory” *J. Fluid Mechanics* **275** 157-199.
5. Phillips, R.J., R.C. Armstrong, R.A. Brown, A.L. Graham, and J.R. Abbott, 1992 “A Constitutive Equation for Concentrated Suspensions that Accounts for Shear-Induced Particle Migration” *Phys. Fluids A* **4** (1) 30-40.
6. Validyne Corp.: www.validyne.com
7. Arris, H., 2000, private communication

6 Appendix: Experimental Results

A summary and graphical presentation of the experiments is given here. The electronic pressure/time data and the video images in .avi format are available from the author. This appendix is divided into four sections, covering

A.1: single-fluid particle-free encapsulations
A.2: dual-fluid particle-free encapsulations
A.3: dual-suspension particle-filled encapsulations
A.4: a summary of mold level vs. time for experiments where this was available

Conditions of the encapsulation are given, with comments where applicable for A.1-A.3. Pressure vs. time curves for the differential pressures within the mold and for the mold vacuum are given. The figure below is a guide to be used with the plots of A.4

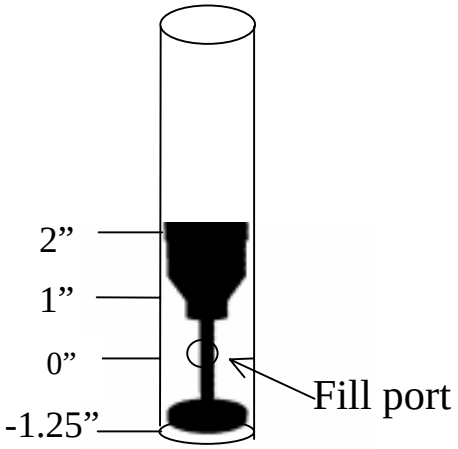

Figure A.1 Locations corresponding to plots of Appendix A.4

Note 1: The transducers, ΔP_1 and ΔP_2 can be connected to either span. See the appendix tables for details.
Note 2: Level locations to the left of the drawings correspond to the locations of the figures in Appendix A.4. Time zero is the time at which the fluid level is at location 0. The floor of the mold is 1.25 inches below the fill port.

A.1 Single Fluid Particle-Free Mold Fills

Single Fluid 7-201

Run ID:	Fill 7-201	**Notes**
Date:	07/20/2000	
Fluid:	86.2 % glycerol	Lag in pressure response relative to stopwatch value. Short tubing used. One-inch profile pressure dip unexplained.
Density	1.226 g/ml	
Transducer 1 location:	2" port	
Transducer 2 location:	1" port	
Calibration Constant (psi/mV)		
#1:	0.0068	
#2:	0.0053	
Movie	Fill7201.avi	

Fill 7-201

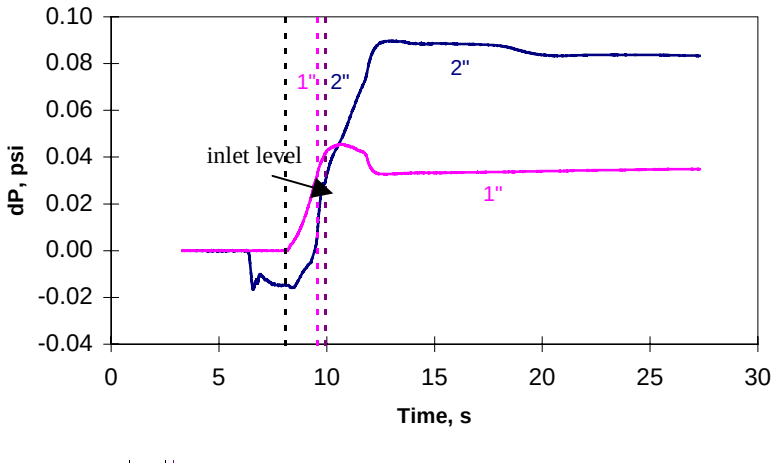

Vessel Pressure, Fill 7-201

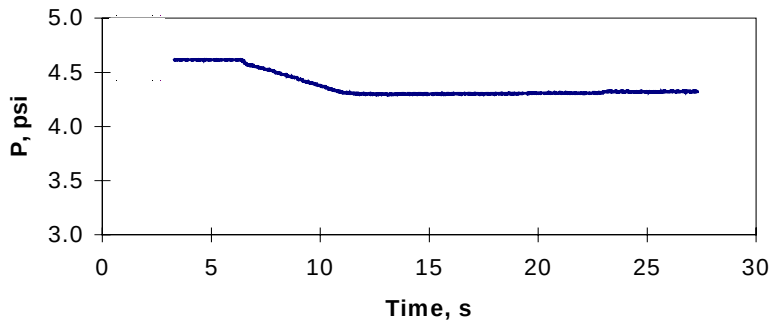

Single Fluid 7-212

Run ID:	Fill 7-212	**Notes**
Date:	07/21/2000	
Fluid:	86.7 wt % glycerol	Vessel pressure dropped, causing obvious dip immediately after fluid enters vessel, but good pressure profile for 2" stretch, good time synchronization. (movie not informative)
Density	1.226 g/ml	
Transducer 1 location:	2" port	
Transducer 2 location:	1" port	
Calibration Constant (psi/mV)		
#1:	0.0068	
#2:	0.0053	
Movie	Fill7-212.avi	

Fill 7-212

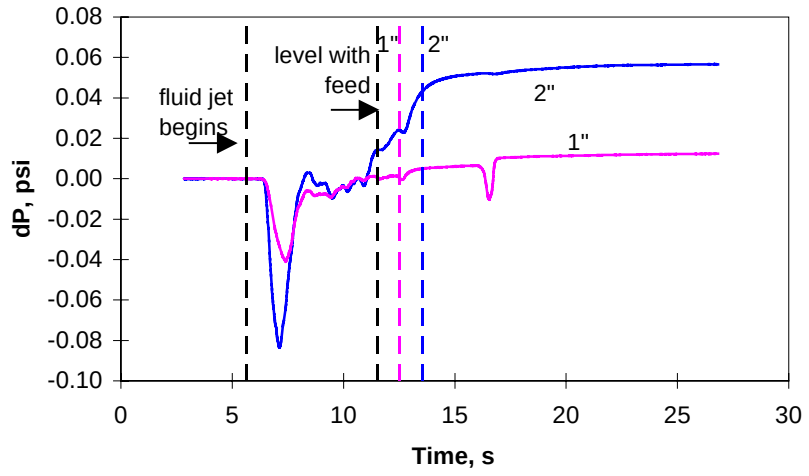

Vessel Pressure

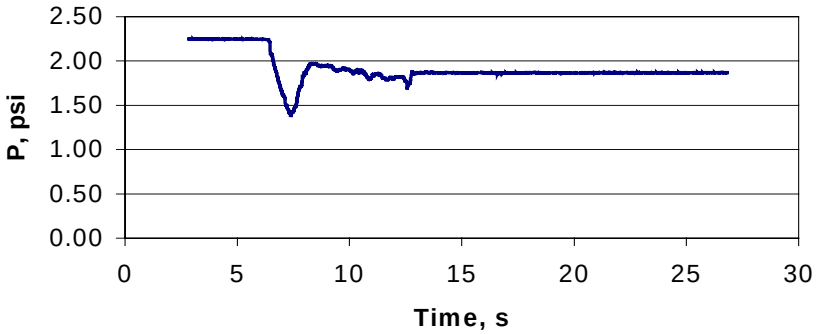

Single Fluid Fill 7-131

Run ID:	Fill 7-131	**Notes**
Date:	07/13/2000	
Fluid:	100 % glycerol	Vessel pressure dropped, causing obvious dip immediately after fluid enters vessel, but good pressure profile for 2" stretch, good time synchronization.
Density	1.261 g/ml	
Transducer 1 location:	2" port	
Transducer 2 location:	1" port	
Calibration Constant (psi/mV)		
#1:	0.0068	
#2:	0.0053	
Movie	no movie	

Fill 7-131

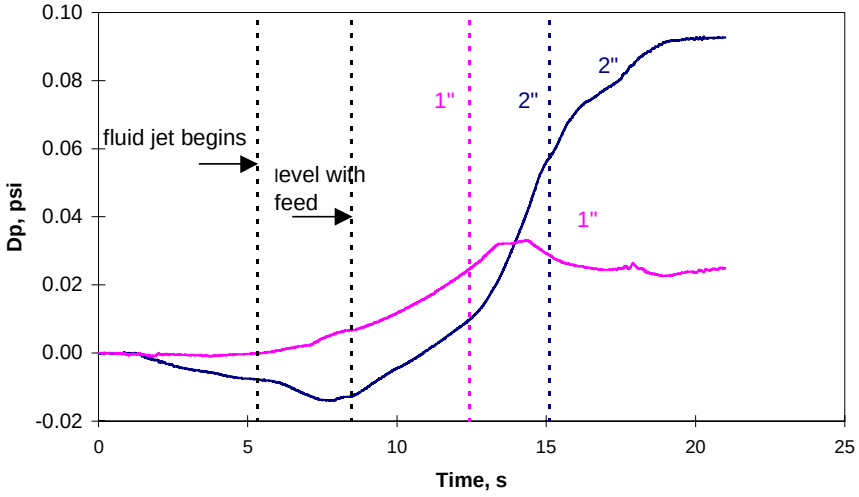

Vessel Pressure, Fill 7-131

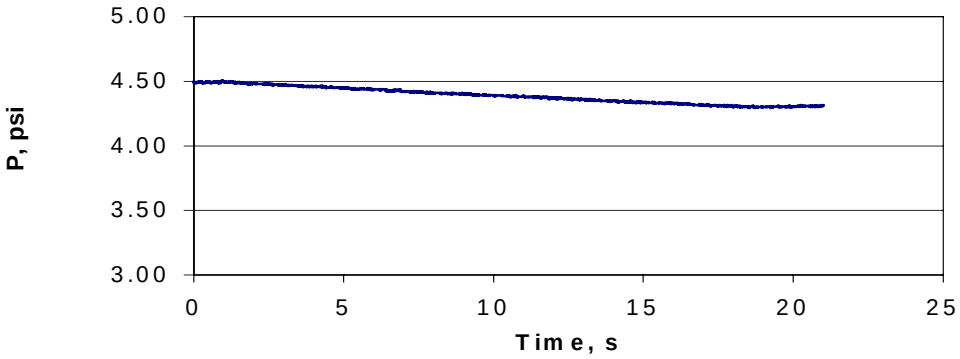

Single Fluid Fill 7-213

Run ID:	Fill 7-213	**Notes**
Date:	07/21/2000	
Fluid:	100 % glycerol	Lost intermediate times
Density	1.261 g/ml	
Transducer 1 location:	2" port	2” span only
Transducer 2 location:	1" port	
Calibration Constant (psi/mV)		
#1:	0.0068	
#2:	0.0053	
Movie	Fill7-213.avi	

Fill 7-213

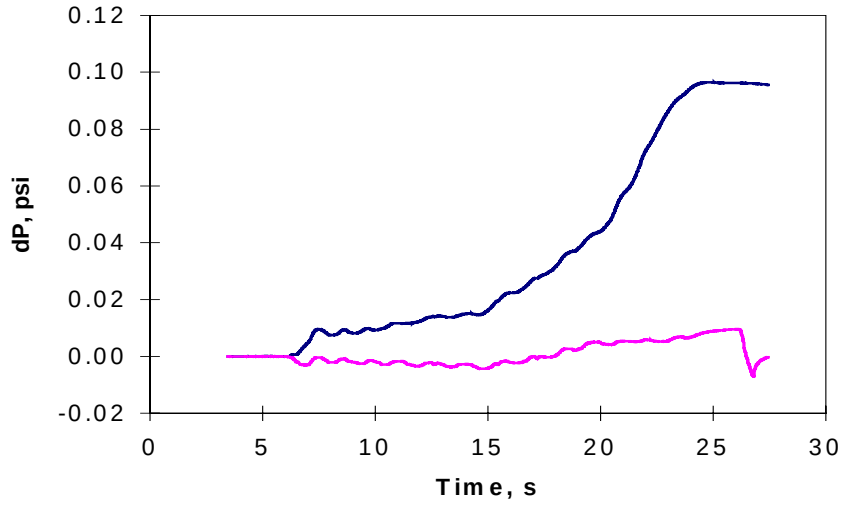

Vessel Pressure, Fill 7-213

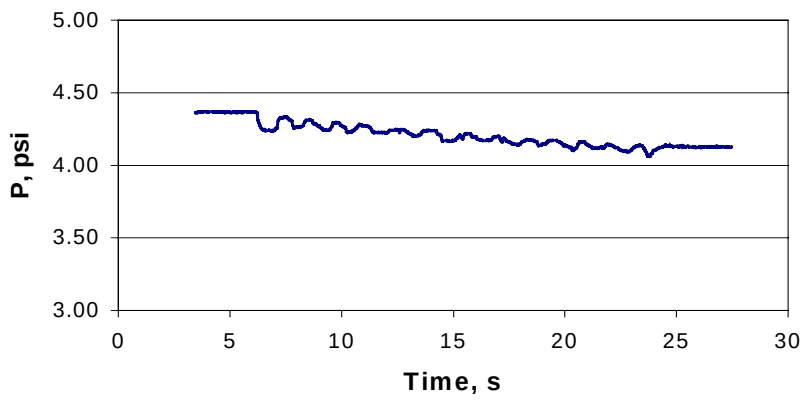

A.2 Two Fluid Particle-Free Mold Fills

Two-Fluid 7-221

Run ID:	Fill 7-221	**Notes**
Date:	07/22/2000	
Lower Fluid:	UCON/$C_2H_2Br_4$	1" span did not form good trace.
Upper (fill) Fluid:	100% glycerol	
Density, g/ml	1.2611	
Transducer 1 location:	2" port	Good synchronization with pressure spike.
Transducer 2 location:	1" port	
Calibration Constant (psi/mV)		
#1:	0.0068	
#2:	0.0053	

Fill 7-221

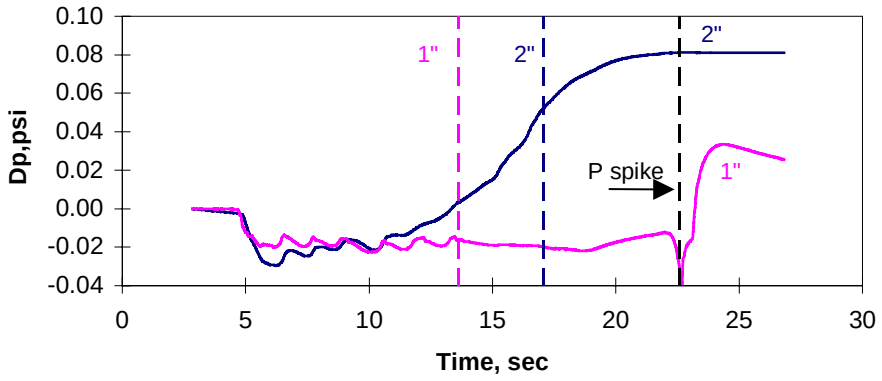

Vessel Pressure - Fill 7-221

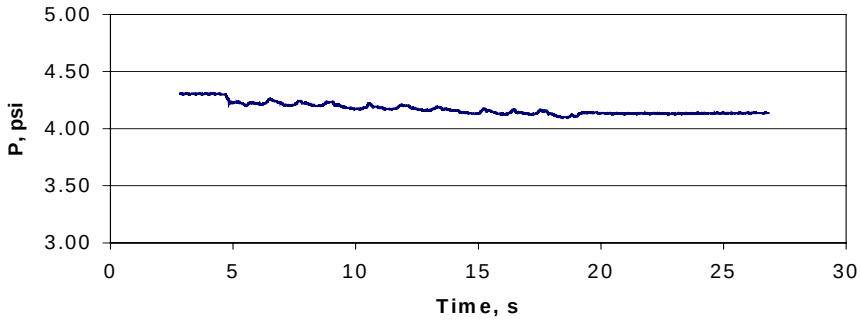

Two-Fluid 7-121

Run ID:	Fill 7-121	**Notes**
Date:	07/12/2000	
Lower Fluid:	UCON/$C_2H_2Br_4$	
Upper (fill) Fluid:	100% glycerol	
Density, g/ml	1.2611	
Transducer 1 location:	1" port	
Transducer 2 location:	2" port	
Calibration Constant (psi/mV)		
#1:	0.0135	
#2:	0.0126	
Movie	Fill7-121.avi	

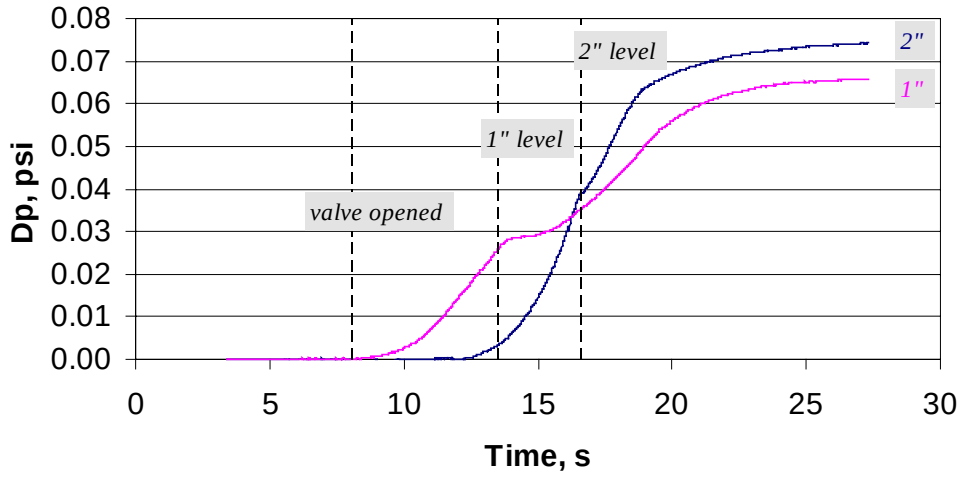

Vessel Pressure, Fill 7-121

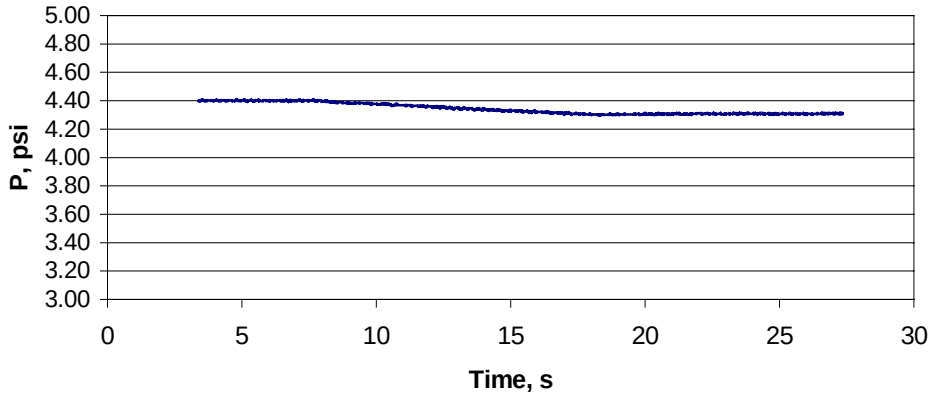

Two-fluid 8-111

Run ID:	Fill 8-111	**Notes**
Date:	08/11/2000	
Lower Fluid:	UCON/$C_2H_2Br_4$	Data from
Upper (fill) Fluid:	100% glycerol	diaphragm #2
Density, g/ml	1.2611	#1 for pressure
Transducer 1 location:	2" port	spike (timing)
Transducer 2 location:	1" port	only.
Calibration Constant (psi/mV)		
#1:	0.0068	
#2:	0.0096	
Movie	Fill8-111.avi	

Fill 8-111

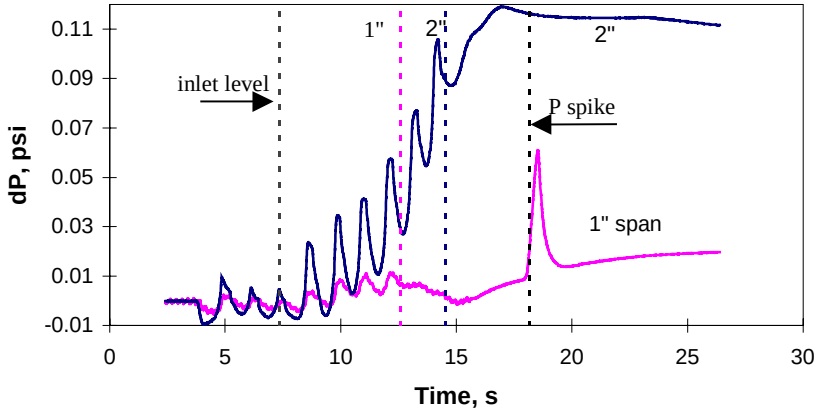

Vessel pressure Fill 8-111

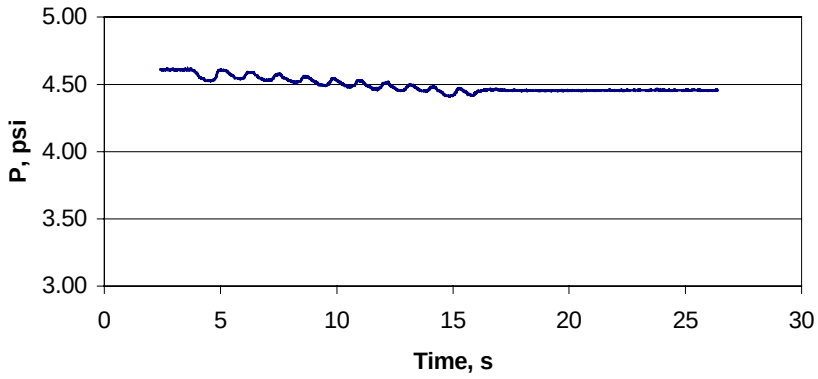

Two-Fluid 8-112

Run ID:	Fill 8-112	**Notes**
Date:	08/11/2000	
Lower Fluid:	UCON/$C_2H_2Br_4$	1" span did not respond until pinch. After pinch, it returned to expected hydrostatic value
Upper (fill) Fluid:	100% glycerol	
Density , g/ml	1.2611	
Transducer 1 location:	2" port	
Transducer 2 location:	1" port	
Calibration Constant (psi/mV)		
#1:	0.0068	Good 2" profile. Synchronization with pressure spike good.
#2:	0.0096	
Movie	Fill8-112.avi	

Fill 8-112

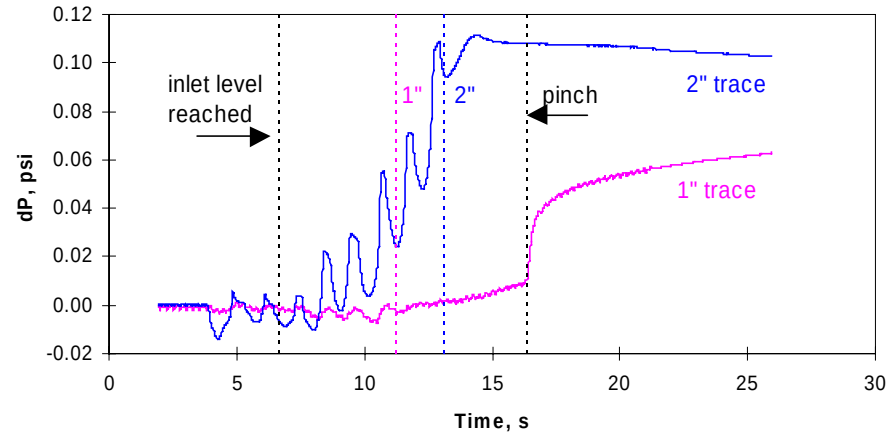

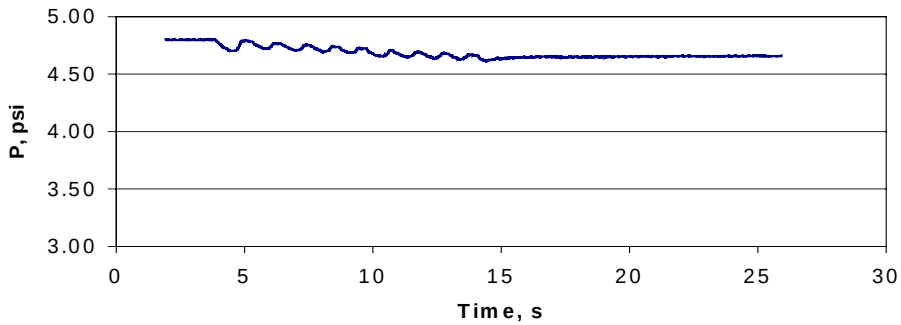

A.3 Two Fluid Mold Fills with Particles

Suspension 6-71

Table 2

Run ID:	Fill 6-71	**Notes**
Date:	06/7/2000	
Lower Suspension:	ALOX/ 80% glycerol	Data collected for 16 seconds, most of fill not captured
Density (lower), g/ml	1.473	
Upper (fill) Suspension:	SiO2/ 87.6 % glycerol	Good agreement of pressures at each port
Density (upper), g/ml	1.26	
Transducer 1 location:	1" port	Prior to fluid reaching fill port, slow drop in pressure, followed by recovery.
Transducer 2 location:	2" port (DP15-22)	
Calibration Constant (psi/mV)		
#1:	0.00317	
#2:	0.01357	
Movie	Fill6-71.avi	

Fill 6-71

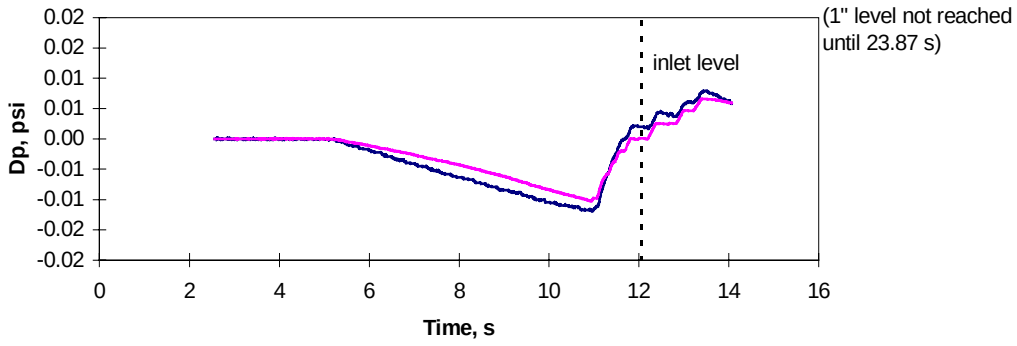

Vessel Pressure History

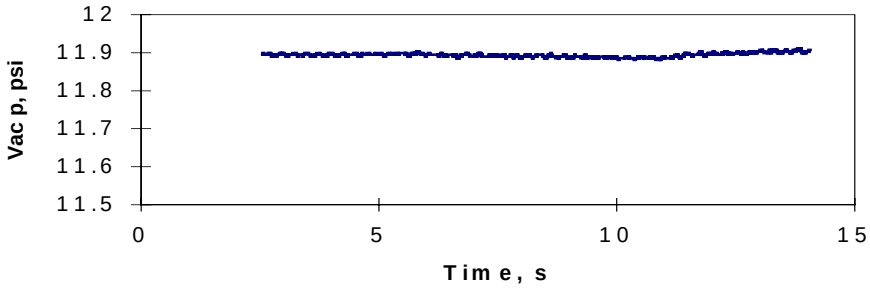

A.4 Fill Profiles (Level vs. Time) See Figure A.1, p.23 for guide

Note: Time zero refers to time at which level is at 0 mark of Figure A.1. Dashed line indicates estimation was used based on known time of initiating pressure collection data.

Fill 7-201 Fill Profile

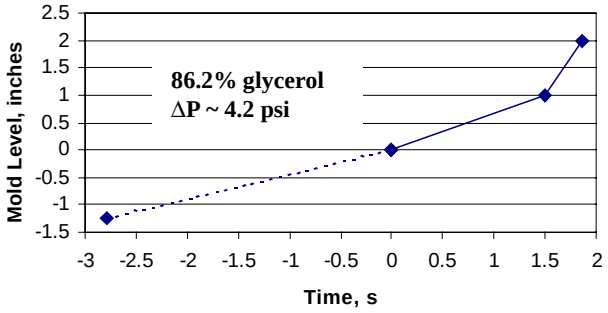

Fill 7-212 Fill Profile

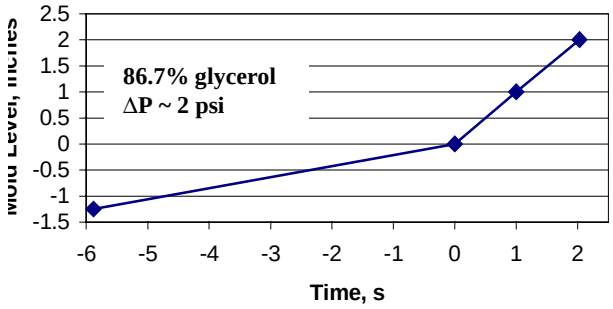

Fill 7-131 Fill Profile

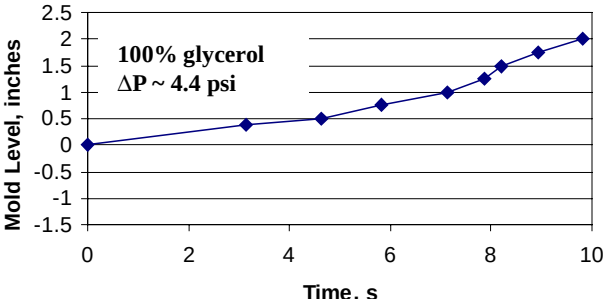

Fill 7-121 Fill Profile

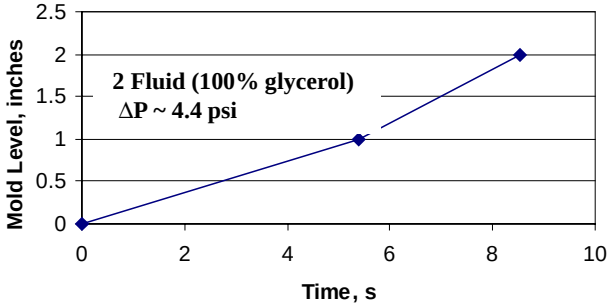

Fill 8-111 Fill Profile

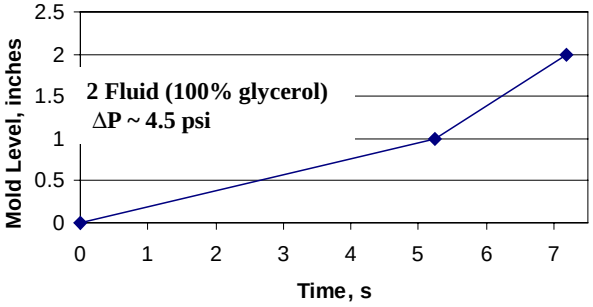

Fill 8-112 Fill Profile

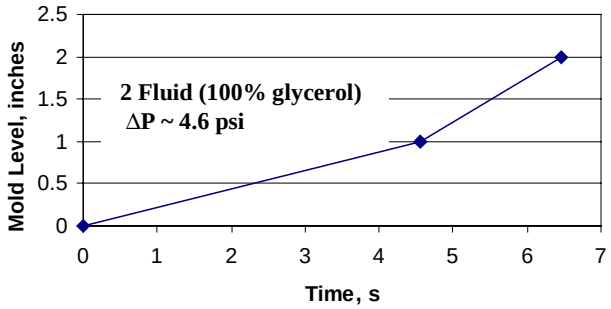

Fill 6-71 Fill Profile

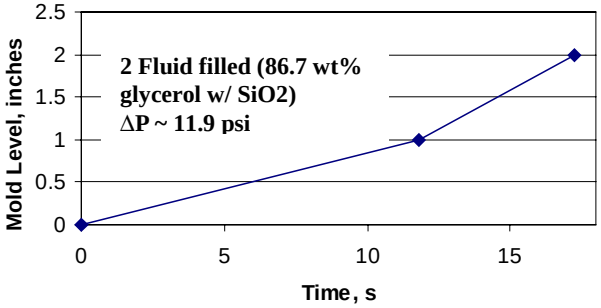

Distribution

MS 0719	E. Lindgren, 6131
MS 0828	A.C. Ratzel, 9110
MS 0828	J. Moya, 9130
MS 0828	M. Pilch, 9133
MS 0834	M.R. Prairie, 9112
MS 0834	T.J. OHern, 9112
MS 0834	K.A. Shollenberger, 9112
MS 0836	C. Romero, 9116 (5 copies)
MS 0834	R.R. Rao, 9114
MS 0834	L.A. Mondy, 9114
MS 0834	T.A. Baer, 9114
MS 0834	J.J. Johannes, 9114
MS 0836	E.S. Hertel, 9116
MS 0841	T.C. Bickel, 9100
MS 0958	H. Arris, 14172
MS 0958	M. Donnelly, 14172
MS 1411	R. Lagasse, 1811
MS 0612	Review & Approval Desk, 9612
MS 0899	Technical Library, 9616 (2 copies)
MS 9018	Central Technical Files, 8945-1